Journal of Multidisciplinary Sciences
www.multidisciplines.com

Glauconite as a geological natural material for phosphate removal from groundwater at Abu Minqar area, El-Farafra Oasis, Egypt

Mahmoud Hamed Darwish[1]* and Dalal Zein El-Ab deen Husein[2]
[1]Geology Department, Faculty of Science, New Valley University, El-Kharga, 72511, Egypt.
[2]Chemistry Department, Faculty of Science, New Valley University, El-Kharga, 72511, Egypt.
**Corresponding author email address: mahmoud.hamed68@sci.nvu.edu.eg*

Received: 25 December 2020; Accepted: 05 February 2021; Published online: 10 February 2021

Abstract. The main aim of this study is to treat the presence of phosphate in groundwater. Twelve groundwater samples were selected and collected from the Abu Minqar wells, El-Farafra oasis, Egypt. Physic-chemical parameters as EC, pH, and TDS is measured. Major ions as Na^+, Mg^{++}, Ca^{++}, K^+, Cl^-, SO_4^{--} and HCO_3^-, and minor ions as Fe^{++}, Mn^{++}, and PO_4^{---} is determined. The obtained results show that the concentration of these ions in groundwater reflects water-bearing sediments. Treatment of groundwater contaminated with phosphate includes purification steps, which can be difficult to introduce to rural regions where sophisticated applications are not feasible with a technological and financial framework. The use of different local abundance adsorbents in these areas can be an option. In this research, glauconite, as a natural geological material adsorbent, is used to remove phosphate from groundwater. Combined impacts on the operating parameters, including initial concentration, adsorbent dose, and contact time, were investigated. At a contact period time of 50 min, the maximum phosphate adsorption (89.1% removal and 12.82 mg/g) was achieved at an initial phosphate concentration of 50 mg/L and a glauconite dose of 0.1 g. The experimental data were revealed that Langmuir and Temkin Isotherms described the removal process, and the pseudo-second-order kinetic model fits well the removal process, with a correlation value of $R^2 = 0.99$. Moreover, the results conducted that glauconite material could potentially be applied to remove phosphate from groundwater.

Keywords: Geology, glauconite, phosphate, groundwater, chemical analysis, adsorption, El-Farafra oasis, Egypt

Cite this as: Darwish, M.H. & Husein, D.Z.E. (2021). Glauconite as a geological natural material for phosphate removal from groundwater at Abu Minqar area, El-Farafra Oasis, Egypt. J. Multidiscip. Sci. 3(1), 1-15.

1. Introduction

The groundwater wells selected for this study to remove phosphate are located in the Abu Minqar area, southwest of El-Farafra Oasis, Egypt (Figure 1). The study of the geological situation is necessary for assessing environmental problems and water quality of any region (Darwish & Galal, 2020; Galal & Darwish, 2020; Darwish et al., 2020). The quality of groundwater affects when the water flows in pores, joints, and cracks of the water-bearing sediments. Chemical analysis of groundwater is necessary for water resources management and environmental impacts on the groundwater (Farrag et al., 2019). The most topic in the world is water quality low because of many naturals and anthropogenic activities. Geological and geochemical processes, land to use, infiltration rate, and human activities are the most factors affecting groundwater quality (Freeze & Cherry, 1979). Recently, the quality of groundwater has deteriorated in Egypt (Ali & Bin Obaidat, 2010). Cation exchanges with surrounding geological layers, mineral dissolution and sedimentation, and evaporation, oxidation, and reduction operation, are sources of the chemical content of groundwater, which helps to know the various factors that affect the quality of groundwater (Aly et al., 2016). Major ions and trace elements content of groundwater determines its suitability for different purposes (Adhikary et al., 2012; Kaitantzian et al., 2013; Elkrail & Obied, 2013).

Water pollution with phosphates comes from natural and anthropogenic phosphate sources. Runoff, subsurface infiltration, rocks and minerals decomposition, inorganic materials weathering, sedimentation operation, and deposition by the atmosphere

are the natural sources of phosphate in water pollution. Phosphate mining, fertilizers, wastewater, animal wastes, detergents, industrial discharge, and drinking water treatment are the most anthropogenic sources of phosphate in water contamination (Spraill et al., 1998; Sheila, 2005). Natural phosphate levels in water are not harmful to human health, animals, or the environment, but very high levels can cause digestive problems (Sheila, 2005). The high percentage of phosphorus in water can cause increased growth of algae, which can result in decreased levels of dissolved oxygen that leads to eutrophication. Also, high levels lead to algae blooms that produce algal toxins, which can be harmful to human and animal health (Brian, 2005).

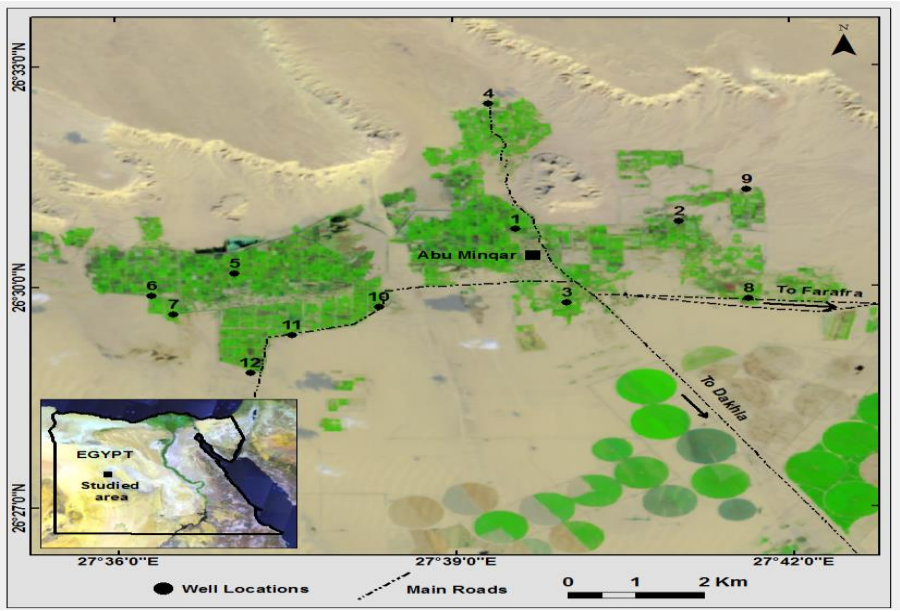

Figure 1. Location map of the studied area and groundwater wells.

Glauconite is almost found in sediments, sandstones, and carbonates. In descriptions of sedimentary rocks, glauconite is a good remarked bed and used to distinguish stratigraphic layers in the geological maps. McRae (1972) defined glauconite as a green, Fe-K-rich micaceous mineral with a 2:1 dioctahedral illite-like structure. It is made of inter-stratification of non-expandable (10 Å) and expandable Fe-smectite layers. In Egypt, the sedimentary sequence, which contains glauconite deposits, is found at Bahariya Oasis and Abu Tartur plateau in the Western Desert at four different rock units; Bahariya Formation (lower Cenomanian age), Qusseir Formation (lower-middle Campanian age), Duwi Formation (upper Campanian age), and Hamra Formation (Lutetian-Bartonian Age). Glauconite as the age of lower Cenomanian, upper Campanian, and Lutetian-Bartonian, occur as pellets, while glauconite as lower-middle Campanian age occurs as fine-grained particles (Baioumy et al., 2020). The sample of glauconite, which was used in this research collected from the Abu-Tartur phosphate mining area. The geological section in this area consists of some rock units from base to top: Quseir, Duwi, Dakhla, and Kurkur Formations. Glauconite is found in the upper member of the Duwi Formation and is composed of glauconite sandstone intercalated with sandstone and shale with a thickness of about 3 m (Baioumy & Tada, 2001).

2. Geological setting

According to CONOCO (1987) and Hermina (1990), the area of Abu Minqar and its surrounding has sedimentary rocks ranging in age from upper Cretaceous to Quaternary. The outcrop geological section consists of many rock units such, Quseir, Duwi, Khoman, Dakhla, Tarawan, Garra, Esna, Farafra, and Minqar El Talh Formations and aeolian sand and playa deposits (Figure 2). The Quseir Formation is composed of varicolored shale, siltstone, and sandstone (Campanian age), and it follows by the Duwi Formation. Dewi Formation is composed of phosphate beds alternating with black shale and glauconite sandstone (Campanian - Maastrichtian age). Khoman Formation is composed of massive neritic white chalk and chalky limestone (Campanian - Maastrichtian). Dakhla Formation covers the floor of the Abu Minqar depression. Dakhla Formation comprises open marine shale with calcareous, sandy, and phosphate intercalation (Early Paleocene age). Tarawan Formation is composed of white chalk,

impure limestone, or dolomite (Early Paleocene age). Garra Formation is composed of white chalky limestone, occasionally siliceous (Paleocene age). Esna Formation is composed of Greenish-grey open marine shale, and the upper part represents limestone facias (Late Paleocene – Early Eocene age). Farafra Formation is represented by white to grey alveolinid lagoonal limestone (Eocene age). Minqar El Talh Formation is formed into continental to lacustrine sandstone with siltstone (Post-Miocene age). Aeolian sand and playa deposits (Quaternary deposits), Aeolian sand forms scattered dunes or sand sheets along the Farafra depression floor and the plateau surface, playa deposits composed of fine sand, silt, and dark brown clay mixed with gypsum and halite and rich with plant remains.

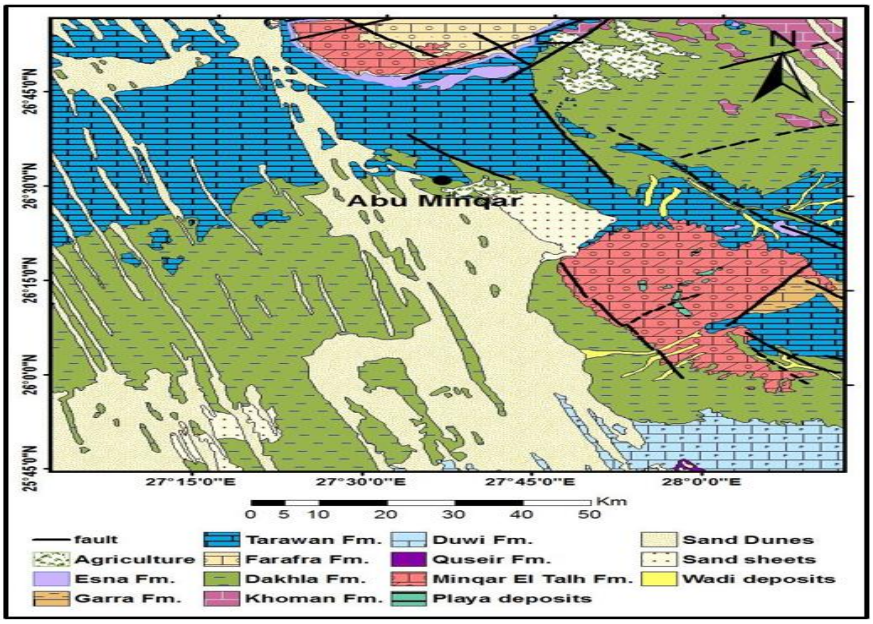

Figure 2. Geologic map of the area (modified after CONOCO, 1987 and Hermina, 1990).

3. Hydrogeological setting

Groundwater is the single source of water in the study area for domestic, and irrigation uses. El-Farafra Oasis belongs to the great NSAS that covers vast areas of Egypt. Many authors described the hydrogeological situation of the aquifer (Ebraheem et al., 2002; Ebraheem et al., 2003; Elsheikh, 2015; Mahmod et al., 2013; Shata, 1982; Voss & Soliman, 2014). According to them, The Nubian sandstone aquifer with an average thickness varies from 2525 to 2675 m is the primary source of groundwater in El-Farafra oasis. The depth of wells ranges from 350 to 1200 m. NSAS comprises a thick sequence of coarse sandstone and sandy clay interbedded with shale and clay beds. The aquifer horizons constitute sandstone beds, while the low conductivity layer of shale interbeds causes the slow vertical movement of the groundwater between the aquifer layers.

Two aquifers represent the groundwater bearing horizons in the studied area. The Post Nubian succession represents by 220 m thicknesses of shale, limestone, and dolomitic limestone. The NSAS is the main water-bearing horizon and consists of alternating sand and shale layers. The sand units form the water-bearing horizons, while the shale layers constitute an aquiclude separating them. In the Western Desert of Egypt, the Post-Nubian sandstone aquifer system is north of latitude 26° (CEDARE, 2001). Figure 3 shows a hydrogeological cross-section from the south to the north direction in El-Farafra oasis. The aquifer is composed of successive thick sandstone beds intercalated with thin shale and clay beds. Two thick sand zones, the first zone with depth ranges between 300 and 500 m below ground surface, the second zone with a depth range between 600 and 1200 m below ground surface. In the hydrogeological cross-section, wells 1 and 13 are located at the Abu Minqar area and show the water-bearing sediments and faults under the area. Water-bearing sediment plays a significant effect role in the chemical content of the groundwater. The fault structure may allow the water to move vertically through the rock layers. Water dissolves the chemical content of the sediments and adds to the chemical content of the groundwater.

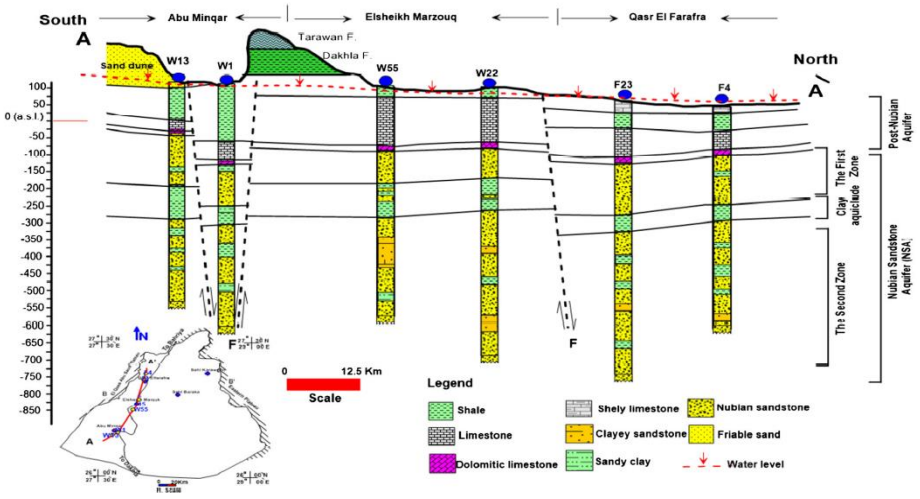

Figure 3. Hydrogeological cross-section from south to north through El-Farafra Oasis (Elsheikh, 2015).

4. Materials, methods and characterization

Twelve groundwater samples were collected from twelve underground wells in the study area, and their chemical analysis was carried out in the central laboratory, El-Kharga, New Valley, Egypt. The data includes the measured TDS, EC, pH, and determined concentration of significant ions Na^+, K^+, Ca^{++}, Mg^{++}, HCO_3^-, SO_4^{--}, Cl^- and some minor and trace elements PO_4^{---}, Fe^{++} and Mn^{++}. Both EC and pH were measured in the field. Na and K contents were determined using a flame photometer. Ca, Mg, and trace elements are determined employing a spectrophotometer. Chloride and sulfate are determined colorimetrically and bicarbonate by titration method. Sodium Adsorption Ratios (SAR) calculated by the following equation:

$SAR = Na^+ / [(Ca^{2+} + Mg^{2+})/2]^{0.5}$ epm (U.S. Salinity Laboratory Staff, 1954).

The glauconite rock sample was collected from the upper part of the Duwi Formation of the Abu Tartur plateau, El-Kharga, Egypt. The rock sample was crushed and sieved through an appropriate mesh size (75-480) µm. Subsequently, to avoid the moisture from being inputted, the sample was placed in a desiccator before the experiments began. All chemicals used in this study were analytical grade and used without further purification. The fresh glauconite sample's phase and mineralogical composition were done using an X-ray diffractometer (Philips-PW1710), while the surface functional group analysis was performed using FT-IR spectrophotometer (Thermo Fisher-Nicolet iS10).

5. Experimental setup and calculations

In batch modes, each experiment was carried out with the addition of 25 mL of phosphate solution in 100 mL Erlenmeyer flak to 0.1 g glauconites (initials phosphate concentration from 30 mg/L to 150 mg/L and temperature 22 °C). For 180 minutes, the flasks were shaken. The suspensions were centrifuged and filtered immediately using a 0.45 µm filter after shaking the slurries. The filtrate was then treated with ammonium molybdate and ascorbic acid solution until calculating the phosphate concentration on a spectrophotometer (PerkinElmer; LAMBDA 750). Equations (1) and (2) were used to measure the adsorbed and percent removal of phosphate:

$QE = (C_o - C_e)\ V/m$ (1)

$(\text{Removal } \%) = (C_o - C_t)\ /C_o \times 100$ (2)

Where both C_e and C_o are the equilibrium and initial phosphate concentration. V is the volume of the phosphate solution (mL), m is the adsorbent mass (mg).

Various glauconite masses were used to study the adsorbent dose or solid to liquid ratio (S/L) (0.03 to 0.15 g). Pseudo-first order and pseudo-second orders linear kinetic models were used to estimate the rate constants for phosphate adsorption kinetics (Lagergern, 1898). For this reason, in Equation (3), Pseudo-first-order expression is used:

$$\text{Log } (QE-q_t) = \log QE - (K_1/2.303)\, t \quad (3)$$

Where K1 (min^{-1}) is the constant pseudo-first-order rate. Qe (mg/g) and qt (mg/g) are equilibrium and time t adsorbed phosphate.

The pseudo-second-order expression could be described as shown in equation (4) (Mckay & Ho, 1999):

$$t/q_t = 1/(K_2 q_e^2) + (1/q_e)t \quad (4)$$

K_2, (g/mg. min), denoted the constant pseudo-second-order phosphate adsorption rate onto glauconite.

Adsorption isotherms are correlated with an adsorbed phosphate volume of constant temperatures to the equilibrium solution concentration. The most common models to evaluate experimental findings include Temkin, Freundlich, and Langmuir isotherms. The three isothermal models were used for obtaining isothermic adsorption constants. The following equation (5) is used to calculate the Langmuir isotherm (Langmuir, 1918):

$$C_e/QE = (1/q_L K_L) + (1/q_L)\, C_e \quad (5)$$

Where q_L is the phosphate adsorption capacity of glauconite (mg/g), and K_L is the Langmuir constant (mg/L).

Freundlich model was calculated as equation (6) (Freundlich, 1906):

$$\text{Log } QE = \log K_F + (1/n) \log C_e \quad (6)$$

KF and 1/n are Freundlich constants related to glauconite adsorption capacity and the complexity or heterogeneity factor.

Temkin model can be written as:

$$QE = B \ln A + B \ln C_e \quad (7)$$, (Temkin & Pyzhev, 1940)

$$\text{Where } B = RT/b \quad (8)$$

A, (mg/L), and B are known as Temkin constants related to the equilibrium binding and the adsorption heat. R and T are the gas constant and the absolute temperature, respectively.

6. Results and Discussion

The chemical analysis of the collected groundwater samples and the results are given in; Figure 4 and Tables 1 and 2.

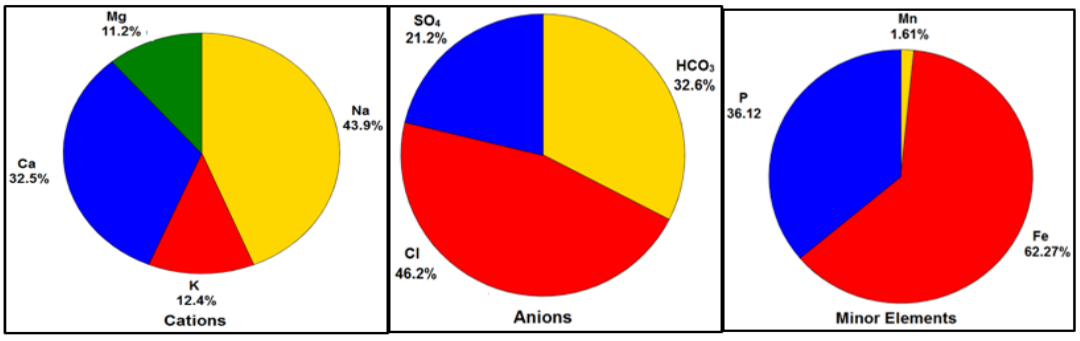

Figure 4. Pie diagram for groundwater composition of the Abu Minqar wells. (https://www.mathsisfun.com/data/pie-charts.html)

Table 1. Physic-chemical analysis of the groundwater samples collected from the Abu Minqar wells.

Well	Cations (mg/L)				Anions (mg/L)			Minor Ions (mg/L)			T.H. mg/L	pH	TDS mg/L	EC (µS/cm)	SAR (epm)
	Na^{+}	K^{+}	Ca^{++}	Mg^{++}	Cl^{-}	Hco_3^{-}	So_4^{--}	Mn^{++}	Fe^{++}	Po_4^{---}					
1	15	5	13	4.4	31	31	20	0.14	5.94	1.80	50.6	6.1	118	196.67	0.9
2	68	15	40	14	154	55	60	0.13	5.66	1.80	157.6	6.2	399	665	2.4
3	13	7	15	5	33	33	21	0.13	5.72	2.20	57.7	6.2	126	210	0.7
4	13.5	6	13.8	4.5	29	35	20	0.08	5.56	2.40	53.0	6	120	200	0.8
5	13	5	20.4	3	26	50	20	0.13	5.24	2.80	63.3	6.2	130	216.67	0.7
6	72	15	38	13	154	53	62	0.14	3.74	2.40	148.5	6.4	400	666.67	2.6
7	12	4	12.8	3.7	21	34	20	0.09	3.82	2.60	47.2	6.6	106	176.67	0.8
8	14.4	5	13.7	5.7	31	33	24	0.15	6.66	2.70	57.7	6.1	125	208.33	0.8
9	14	5	14	5	31	33	20	0.12	0.46	3.40	54.5	6.3	120	200	0.8
10	13	6.4	21	3.8	25	57	22	0.12	6.42	5.04	68.1	6.5	142	236.67	0.7
11	12	6	13	4.5	25	35	20.5	0.14	5.56	5.10	51	6.2	115	191.67	0.7
12	70	14	30	20	155	54	61	0.13	5.74	2.60	157.3	6.5	398	633.33	2.4

EC: Electrical Conductivity **TDS**: Total Dissolved Solids **T.H.**: Total Hardness **SAR**: Sodium Adsorption Ratio

Table 2. The chemical composition of the groundwater in the Abu Minqar wells.

Category	Parameters	Minimum	Maximum	Mean	Standard deviation
Cations (mg/L)	Na^{+} (43.85 %)	12	72	27.49	25.66
	K^{+} (12.42%)	4	15	7.8	4.23
	Ca^{++} (32.51%)	13	40	20.4	10.11
	Mg^{++} (11.22%)	3	14	7.22	5.39
Anions (mg/L)	HCO_3^{-} (32.56%)	31	55	42	10.65
	Cl^{-} (46.20%)	21	155	59.6	57.23
	SO_4^{--} (21.24%)	20	61	27.4	18.21
Minor elements (mg/L)	Fe^{++} (62.27%)	0.46	6.42	5	1.7
	PO_4^{---} (36.12%)	1.8	5.1	2.9	1.1
	Mn^{++} (1.61%)	0.08	0.15	0.13	0.02
	EC (µS/cm)	176.67	666.67	317	204.6
	pH	6	6.6	6.3	0.19
	TDS (mg/L)	106	400	191.6	125.4

6.1. Hydrogen ion concentration (pH)

The pH value is the measure of the activity of hydrogen ions present in water. Surface water and groundwater in direct contact with the atmosphere, the pH value ranges from 7 to slightly more than 8. However, the pH value is a function of CO_2^{-}, CO_3^{--}, and HCO_3^{-} equilibrium, easily disturbed by carbon dioxide content changes. The pH values in the groundwater in the area range of 6 and 6.5, which reflect natural groundwater. The low values of pH are due to the depth of the aquifer from direct contact with the atmosphere.

6.2. The chemical composition of groundwater

Concentrations of minerals and salts in groundwater are higher than in surface waters, especially in areas with an abundance of mineral deposits, areas with the sea, and estuarine water intrusions (WHO, 1979). The type of water-bearing Formations and the surface and subsurface geochemical processes mainly influence the chemical characteristics of groundwater. These processes control the water quality of water movement by increasing or decreasing the dissolved ion contents.

Total dissolved solids (TDS). TDS of the groundwater depends on the type, composition, thickness of water-bearing sediments, and the distance from the recharging sources and varies from less than 100 mg/L to more than 100000 mg/L. TDS value in the study area range of 106 to 400 mg/L. According to Davis and Dewiest (1966) and Hem (1970), the groundwater in the study area is freshwater (less than 1000 mg/ L. TDS values are less than 5000 mg/L in natural water, in brine contains about 300000 mg/L.

Total Hardness (TH). Polyvalent cations, particularly calcium and magnesium, are often found in large concentrations of natural waters. These ions precipitate easily and react with soap to form hard-to-remove scum. The hardness of water relates to its interaction with the soap and the abundance of crusts accumulated in containers or channels, where the water is heating or

transporting. In the study area, the total hardness values range of 47.2 mg/L and 157.6 mg/L. According to Hem (1970), groundwater in the study area is soft to hard.

Groundwater type. From the results of the chemical analysis of the collected groundwater samples and to ion dominance, the abundance sequence of both cations and anions follows the order, $Cl^- > SO4^{--} > HCO_3^-$ and $Na^+ > Ca^{++} > Mg^{++} > K^+$. The water type is Chloride-Sodium. There is a strong relationship between these ions, where the (Na + K)/Cl values range between 0.77 to 1.05 epm.

Sodium adsorption ratio and Electrical Conductivity. In the study area, the SAR values of 0.7 and 2.6 epm, EC values range between 176.67 and 666.67 µS/cm. According to the US Salinity Laboratory Staff (1954), the groundwater in the study area is distinguished from C1 and C2, which denote low to medium conductance, class S1, which denote low sodium adsorption ratio. This means the groundwater in the area is characterized by low sodium water and low to medium salinity water and can be used to irrigate most crops in most soils. According to Richards (1954), the groundwater in the area is excellent for irrigation.

Ions concentrations. Table 3 show the concentration of ions in the groundwater and their sources from rocks and minerals.

Table 3. Sources and normal concentrations of major ions in the groundwater (Module, 1999).

Ions	Sources	Normal Concentration
Sodium	Feldspars, clays, halite, industrial wastes.	High levels often associated with pollution.
Calcium	Amphiboles, feldspars, gypsum, aragonite, calcite, pyroxenes, dolomite, clay minerals.	< 15 mg/L. more than 100 mg/L in carbonate-rich rocks
Magnesium	Amphiboles, olivine, pyroxenes, dolomite, magnesite, clay minerals.	1 to 50 mg/L depending upon rock type
Potassium	Feldspars, feldspathoids, some micas, clays.	Normally, < 10 mg/L
Bicarbonate /Carbonate	Limestone, dolomite.	Bicarbonate: 25 to 400 mg/L. Carbonate < 10 mg/L.
Sulphate	Oxidation of sulphate ores, gypsum, anhydrite.	2 to 80 mg/L.
Chloride	Sedimentary rock, igneous rock.	< 40 mg/L in unpolluted waters

6.2.1. Major ions

Sodium and Potassium. Generally, sodium is found in significant quantities of natural water. Shale and clay sediments often yield water with high sodium content. Other sources of sodium are the leaching of some evaporating such as halite. Sodium concentration on natural waters is less than 200 mg/L, about 10000 mg/L in seawater, and 25000 mg/L in brine (Todd, 1980). Natural sources of potassium in sedimentary rocks are clay minerals, and its concentration is less than 10 mg/L in natural freshwaters (Module, 1999). Potassium concentrations are less than about 10 mg/L in normal waters, 100 mg/L in hot springs, and 25000 mg/L in brine (Todd, 1980). In the study area, sodium represents the main predominant cation, and its value ranges from 12 to 72 mg/L as a percentage of 43.85% from the cations, while the concentration of potassium is between 4 and 15 mg/L as a percentage of 12.42% from the cations.

Calcium. Calcium is founding in carbonates such as limestone and dolomite and sulfates such as gypsum and anhydrite. Water can dissolve up to 600 mg/L of calcium at room temperature from gypsum (Hem, 1989). The calcium concentration of normal water is usually less than 15 mg/L, more than100 mg/L in carbonate-rich rocks (Module, 1999). In general, the calcium concentration of natural water is less than 100 mg/L, but in brine may contain 75000 mg/L (Todd, 1980). The calcium concentration of the groundwater in the study area ranges from 13 to 40 mg/L with a ratio of 32.51% from the cations.

Magnesium. Magnesium is similar to calcium as a principal cation in the surface and groundwater and cause of water hardness. It may be the dominant cation in the groundwater if the aquifer contains dolomite or Mg-rich evaporates. Magnesium occurs as magnesite and other carbonates, sometimes mixed with calcium carbonate and clay minerals. Dolomite contains calcium and magnesium in equal amounts. Magnesium concentration of natural water usually ranges between 1 and 50 mg/L depending upon the rock type (Module, 1999). Generally, the Magnesium concentration of natural water is less than 50 mg/L, in ocean water more than 1000 mg/L, and in brine 57000 mg/L (Todd, 1980). The magnesium concentration of the groundwater in the study area ranges between 4.4 and 20 mg/L as a percentage of 11.22% from the cations.

Bicarbonate. The sources of carbonates and bicarbonate include; carbon dioxide from the atmosphere and produced by organisms in the soil or by the activity of sulfate depressants and other bacteria in deep Formations, various carbonate rocks, and minerals (limestone and dolomite). The concentration of bicarbonate in nature waters ranges from 25 to 400 mg/L (Module, 1999). The bicarbonate concentration of natural water is less than 500 mg/L, and more than 100 mg/L in water is highly charged with carbon dioxide (Todd, 1980). The bicarbonate concentration of the groundwater in the study area ranges between 31 and 55 mg/L as a percentage of 32.56% from the anions.

Sulfate. Gypsum and anhydrite in natural waters are the most sources of sulfates. Usually, the sulfate concentration of normal water ranges between 2 and 80 mg/L (Module, 1999). This concentration is less than 300 mg/L, 200000 mg/L in brine (Todd, 1980). In the study area, the sulfate concentration ranges between 20 and 61 mg/L as a percentage of 21.24% from the anions.

Chloride. The primary sources of chloride in groundwater are evaporated, salty connate water, and marine water. Chloride is present in all-natural waters with an average concentration of 3 mg/L in rainwater and up to 19000 in seawater (Correns, 1956). Although chloride is dissolved from rocks and soil, its presence may indicate contamination by human and animal sewage. Typically, chloride concentration of unpolluted waters is less than 40 mg/L (Module, 1999). This chloride concentration is less than 10 mg/L in humid regions, 1000 mg/L in more arid regions, 19300 mg/L in seawater, and 200000 mg/L in brine (Todd, 1980). In the study area, the chloride values range of 21 and 155 mg/L as a percentage of 46.20% from the anions, and from the chemical analysis results, it is noticed that the high value of sodium, also the high value of chloride, may indicate that the water-bearing sediments containing some halite deposits.

6.2.2. Minor ions

Many elements are present in groundwater in low concentration (less than 0.1 mg/L) but sometimes much higher (Fe^{++}, Mn^{++}, and PO_4^{---}).

Iron. The primary sources of iron in groundwater are the dissolution of iron-bearing minerals commonly found in aquifer sediments as pyrite, siderite, magnetite, and iron silicate. The standard form of groundwater is the soluble ferrous ion (Fe^{++}) oxidized to the insoluble ferric state (Fe^{+++}) when exposed to the atmosphere and precipitates as ferric hydroxide, causing a brown discoloration of the water. Corrosion of suitable casing and other pipes may also contribute iron to the groundwater. Moreover, bacteria activity also increases or decreases the iron concentration of groundwater. The chemistry of iron in natural water is influenced by certain microorganisms (Hem, 1989). The presence of iron in drinking water leads to a metallic taste, so the maximum concentration for drinking water should be 0.3 mg/L (US Public Health Service, 1962). Generally, iron concentration is less than 0.50 mg/L in water. Acid waters from thermal springs, mine wastes, and industrial wastes may contain more than 6000 mg/L (Todd, 1980). White (1963) detected the average iron contents estimated for water derived from different types of sedimentary rocks as sandstone (0.74 mg/L), loose sand (0.31 mg/L), siltstone, and clay (1.61 mg/L), and limestone and clay (0.42 mg/L). In the study area, the iron values range between 0.46 and 6.42 mg/L as a percentage of 62.27% from minor ions, which reflects the Nubian sandstone groundwater.

Manganese. Manganese resembles iron in its chemical behavior, its occurrence of natural water, and it arises from soils and sediments. Metamorphic, sedimentary rocks, mica biotite, and amphibole hornblende minerals contain large quantities of manganese. In natural water, manganese concentration is usually under 0.2 mg/L, whereas groundwater possesses over 10 mg/L. The maximum concentration of manganese for public water supply is set at 0.05 mg/L (US Public Health Service, 1962), and the maximum limit is 0.5 after WHO (Cox, 1954). Manganese concentration of natural waters is about 0.20 mg/L or less, and the groundwater may contain more than 10 mg/L (Todd, 1980). The manganese values in the study area range of 0.08 and 0.15 mg/L as a percentage of 1.61% from minor ions.

Phosphate. Phosphorous is one of the essential nutrients for nutrition and growth for living organisms. Phosphorous is found in natural water and wastewater in the form of dissolved phosphate. Dissolve phosphorus concentrations of groundwater are low because phosphorus tends to sorb to aquifer sediments and soil and is not easily transported in groundwater (Holman et al., 2008). Generally, it recommends that a PO_4 – P (total) of < 1.0 mg/L for drinking water while the EC issue a guide level of 0.5 mg/L. The

concentration level of phosphate in uncontaminated lakes is 0.01- 0.03 mg/L, 0.025 -0.1 mg/L at which plant growth is stimulated, 0.1 mg/L maximum acceptable for the avoidance of rapid eutrophication, and > 0.10 mg/L high level resulting in accelerated algal growth problems (Brian, 2005). The phosphorus values in the study area range of 1.8 and 5.1 mg/L as a percentage of 36.12% from minor ions.

6.3. Characterization of glauconite

The XRD pattern of the fresh rock sample is demonstrated in Figure 5, which depicted that the sample contained glauconite and quartz as significant phases, along with a potassium-iron-silicate mineral as a minor phase (Singla et al., 2020). Both K_2O and Fe_2O_3 are the main components in fresh glauconite (Selim et al., 2018).

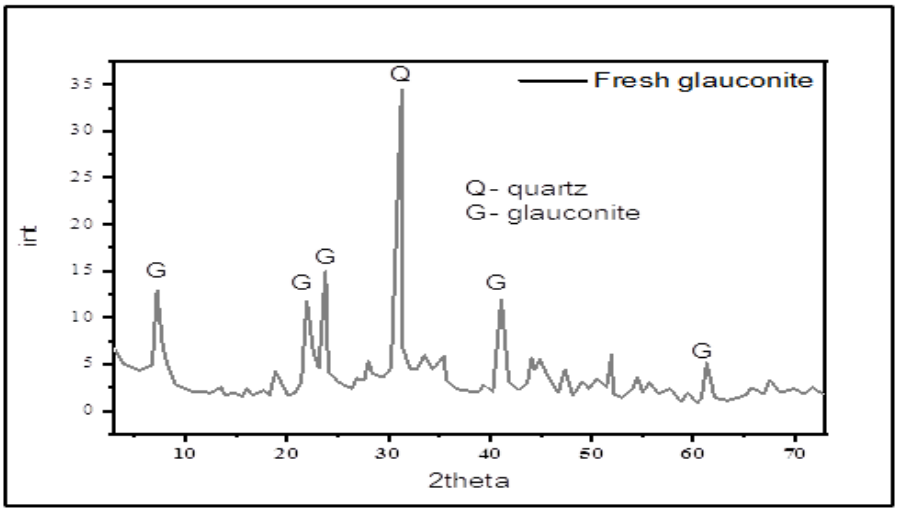

Figure 5. X-ray diffraction of fresh glauconite and its relevant identified minerals.

Figure 6 shows the spectra of the glauconite sample before and after loading with phosphate ions. Before loading with phosphate, the FTIR spectrum confirmed the existence of the interlayer OH stretching vibration band of about 3378 cm^{-1} and the deformation bands at 793 cm^{-1}. The most substantial peaks at about 947 cm^{-1} are attributed to stretching vibration bands of Si-O and Si-O-Fe deformation bands.

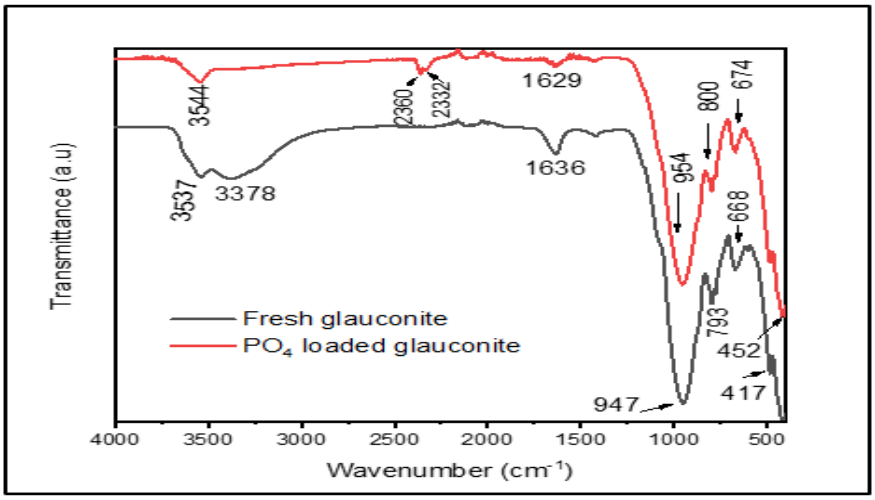

Figure 6. The FT-IR spectra of glauconite before and after loading with phosphate ions.

After loading with phosphate ions, the frequencies of most peaks have been changed and their transmittance intensity. This could be attributed to changes in the chemical structure resulting from the interaction with phosphate ions. As shown in Figure 6, the band that appeared at 668 cm^{-1} in the fresh glauconite is shifted to 674 cm^{-1}, and the peak at 410 cm^{-1} was shifted to 452 cm^{-1}. Moreover, new bands appeared at 2360 and 2332 cm^{-1}, which were attributed to P-H. All such findings confirmed the adsorption of phosphate ions into the surface of glauconite.

6.4. Removal of phosphate using adsorption technique

6.4.1. Effect of glauconite dose on phosphate removal

The adsorbent dose is one of the main factors of the removal process, namely the adsorbent mass to liquid ratio. The adsorbent dose effect was investigated in the range of 1.2-6 S/L to remove phosphate onto glauconite, and the result was stated in Figure 7. With the increase in the S/L ratio, the percentage of phosphate removal increased from 85.02% to 89.02% (S/L=4). After that point (S/L=4), the removal efficiency slightly decreased. On the other hand, the adsorbent mass intake per unit takes the same behavior. It increases as the glauconite dose was raised till S/L ratio=4, then slightly decreased after that point. This finding may be attributed to the more significant number of active sites of glauconite. Hence, S/L=4 is the optimum adsorption dose.

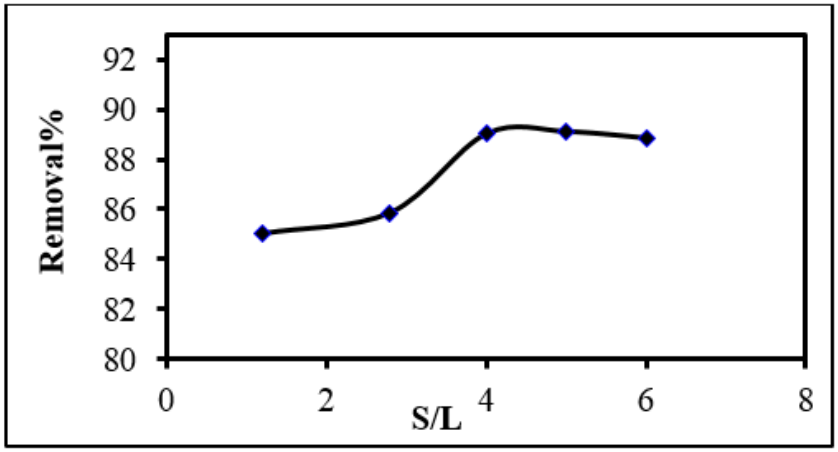

Figure 7. The effect of glauconite dosage on removing phosphate ions (Phosphate concentration = 50 mg/L, temperature =22 °C).

6.4.2. Effect of contact time on phosphate removal

The influence of contact time on the adsorption of phosphate is demonstrated in Figure 8.

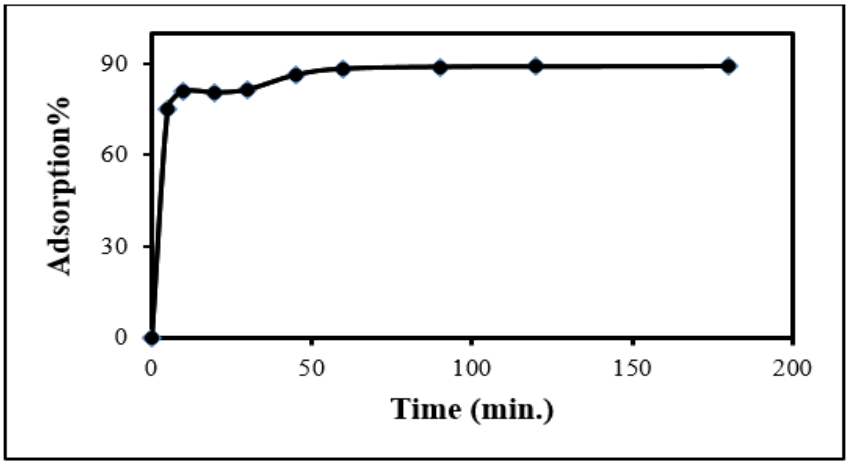

Figure 8. The effect of contact time on phosphate adsorption by glauconite (Phosphate concentration= 50 mg/L, S/L= 4).

The saturation curves in the initial phases increase sharply, indicating that several active sorption sites are accessible. To achieve adsorption equilibrium, around 50 min is required. The glauconite material is ultimately being saturated at this period.

6.4.3. Effect of initial concentration on phosphate removal

Phosphate removal decreased steadily (between 99.4 and 34.1%) while phosphate concentration increases initially (between 30 mg/L and 150 mg/L). Active adsorption sites are likely to be saturated with higher initial levels. The percentage removal, as shown in Figure 9, is based on concentrations (Equation 2). If total quantities are taken into account, the adsorbed quantity also increases to the increased initial concentration (7.4 mg/g to 12.8 mg/g). The driving forces (diffuse gradient) are higher in higher concentrations, and mass to transfer barriers are overcome between aqueous and solid interfaces (Lee et al., 2017).

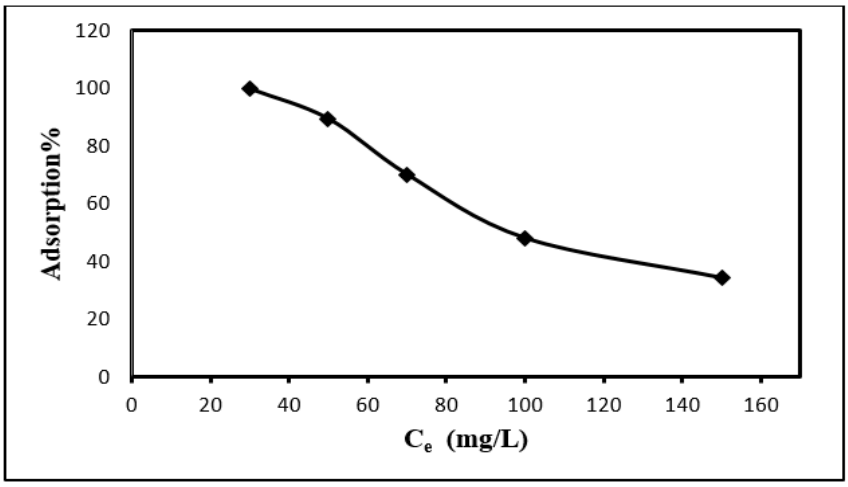

Figure 9. Effect of initial concentration on phosphate removal by glauconite.

6.4.4. Adsorption isotherms

Three isothermic models, Freundlich, Langmuir, and Tempkin, were subject to experimental data from phosphate/glauconite experiments (Figure 10). Isotherm model of Freundlich assumes the adsorption process occurred on a heterogeneous surface, and the adsorbed quantity increases to the increased concentrations of equilibrium. The Langmuir model, on the other hand, assumes a monolayer surface covering. The data obtained in Table 4 with high R^2, Regression coefficient, 0.99, are well-matched with a Langmuir model that describes monolayer adsorption for phosphate by glauconite. The Langmuir isotherm model's R_L separation factor (R_L = 1/ (1+K_L C_{max}), where C_{max} is the highest phosphate concentration) was lower than unity, which also suggested a favorable adsorption mechanism (Husein, 2013).

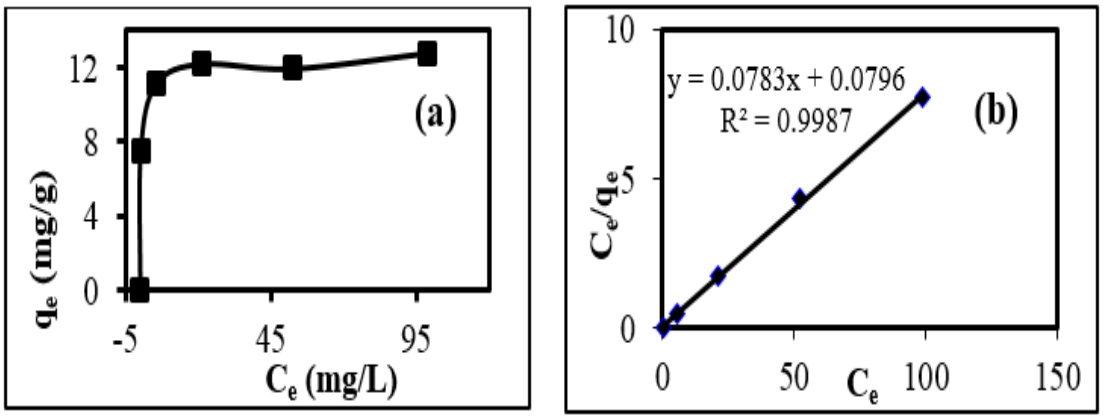

Figure 10. Adsorption isotherm (a) and Langmuir adsorption model (b) for phosphate removal by glauconite.

The Freundlich isotherm's n-value is from 1 to 10 and provides a good predictor for good adsorption (Mekonnen et al., 2020). The Temkin isotherm model was investigated to analyze the adsorption data, and it was found that the R^2 value was 0.95. Therefore, the Temkin model provided an acceptable fit, showing electrostatic interactions between phosphate and glauconite. The Langmuir, Freundlich, and Temkin constant values are presented in Table 4 in tabulated form. Temkin is used to presenting to heat sorption in the energy parameter (B). As shown in Table 1, the value of B (< 20 KJ/mol) suggests that physisorption prevails ion exchange and chemisorptions (Husein, 2019).

Table 4. The calculated parameters of isothermic parameters for phosphate removal by glauconite.

Isotherm model	Parameter		R^2
Langmuir	q_L	12.82	0.99
	K_L	0.99	
Freundlich	K_F	0.97	0.93
	n	2.60	
Temkin	A	87.30	0.95
	B	0.81	

6.4.5. Kinetics studies

Adsorption kinetics is generally studied on the solid/solution interface and, as a function of time, expressed with a solution removal rate. In this research, two kinetic adsorption models test the experimental data, pseudo-first-order, and pseudo-second-order. As shown in Figure 11 and Table 5, the kinetic data is very consistent with the second-order kinetics model. The suitability of glauconite indicates that removing the phosphate from an aqueous solution required chemical interaction (Lee et al., 2015). The calculated adsorption capacity (mg/g) values for the glauconite material (10.99 mg/g) were slightly higher than the experimental value (10.97 mg/g) but not so far, which provides another confirmation on the suitability of the second-order kinetic model.

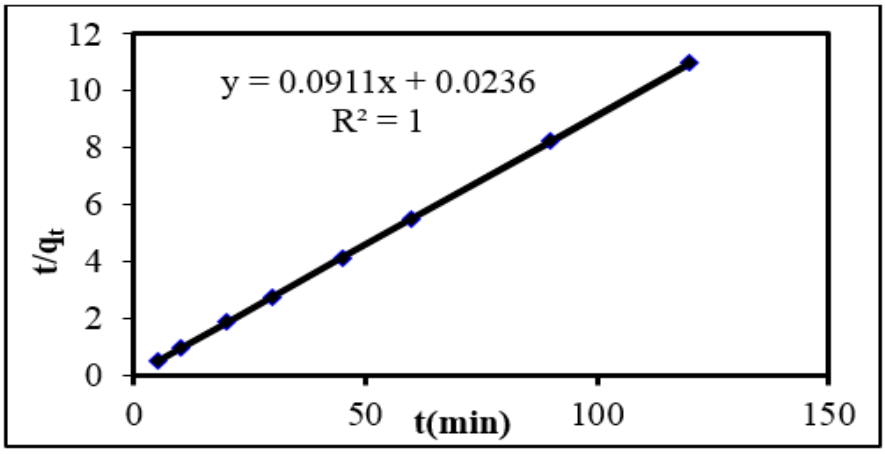

Figure 11. Pseudo-second-order kinetic model for removal of phosphate using glauconite.

Table 5. Pseudo-first and pseudo-second-orders kinetics parameters of phosphate removal onto glauconite.

Kinetic model	Parameter		R^2
Pseudo first order	q_e	0.3	0.619
	K_1	0.03	
Pseudo second order	q_e	10.99	0.99
	K_2	0.36	

7. Conclusion

The chemical composition of the Abu Minqar groundwater wells reflects the water-bearing sediments, the sediments of the aquifer horizons, and the type of sediments between these horizons. The concentration of ions in the groundwater in the study

area is typical for phosphate, iron, and manganese. The concentrations of the trace elements are far high the drinking water permissible limits. The presence of phosphates in water wells in the Abu Minqar area may be due to human activities or through fertilization operations of reclaimed agricultural lands or the phosphate-containing rocks. Glauconite has been used for phosphate removal of groundwater. Glauconite showed an enhanced percentage of phosphate removal of batch mode in a concentration ranges from 30 to 150 mg/L in batch mode. The obtained equilibrium sorption data onto various concentrations showed an appropriate fit to the Langmuir adsorption isotherm, and the sorption capacity determined was found to be 12.82 mg/g. The experimental kinetic data fit the pseudo-second-order model reasonably well. Moreover, sorption data showed that the equilibrium had taken 50 minutes of the contact time, and the removal process is driven by chemisorption. Glauconite could be an effective, cheap alternative adsorbent material to remove phosphate ions from water.

Conflicts of interest. There are no conflicts of interest.

ORCID

Mahmoud Hamed Darwish: https://orcid.org/0000-0002-8930-6422
Dalal Zein El-Ab deen Husein: https://orcid.org/0000-0001-7552-0914

References

Adhikary, P.P., Dash, C.J., Chandrasekharan, H., Rajput, T.B.S. & Dubey, S.K. (2012). Evaluation of groundwater quality for irrigation and drinking using GIS and geostatistics in a peri-urban area of Delhi, India. Arabian Journal of Geosciences, 5, 1423-1434.

Aly, A.A. & Benaabidate, L. (2010). Salinity of water resources in the Siwa Oasis: Monitoring and diagnosis. Water-Rock Interaction. Proceedings of the 13th International Conference on Water-Rock Interaction, WRI-13. p.363-365.

Aly, A.A., Gaber, H.M., Kishk, F.M. & Al-Omran, M.A. (2016). Long-term detection and hydrochemistry of groundwater resources in Siwa Oasis, Egypt. Journal of the Saudi Society of Agricultural Sciences, 15(1), 67-74.

Baioumy, H.M. & Tada, R. (2005). Origin of Late Cretaceous phosphorites in Egypt. Cretaceous Research, 26(2), 261-275.

Baioumy, H.M., Farouk, S. & Al-Kahtany, K. (2020). Paleogeographic, paleoclimatic and sea level implications of glauconite deposits in Egypt: A review. Journal of African Earth Sciences, 171, 103944.

Brian, O. (2005). Phosphate and Water Quality. Wilkes University Center for Environmental Quality, Geo Environmental Sciences and Engineering Department.

CEDARE (2001). Regional Strategy for the utilization of the Nubian Sandstone Aquifer System, Vols 1-4 and annexes 1-2, Center for Environment and Development of the Arab Region and Europe (CEDARE), Cairo, Egypt.

CONOCO (1987). Geological map of Egypt (scale 1: 500,000), compiled by the EGPC and CONOCO Coral, Cairo, Egypt.

Correns, C.W. (1956). The geochemistry of the halogens in physics and chemistry of the earth, Ahvens et. al. (Eds), Mc-Grow-Hill, London, p.181.

Cox, C.R. & WHO (1964). Operation and Control of Water Treatment Processes. World Health Organization (WHO), 49, 375-378.

Darwish, M.H. & Galal, W.F. (2020). Spatiotemporal effects of wastewater ponds from a geoenvironmental perspective in the Kharga region, Egypt. Journal of Progress in Physical Geography: Earth and Environment, 44(3), 376-397.

Darwish, M.H., Megahed, H.A., Farrag, A.A. & Sayed, A.G. (2020). Geo-Environmental Changes and Their Impact on the Development of the Limestone Plateau, West of Assiut, Egypt. Journal of the Indian Society of Remote Sensing, 48, 1705-1727.

Davis, S.N. & DeWeist, R.J.M. (1966). Hydrogeology. John Wiley and Sons, New York, p.463.

Ebraheem, A.M., Riad, S., Wycisk, P., Seifelnasr, A.M. (2002). Simulation of impact of present and future groundwater extraction from the non-replenished Nubian Sandstone aquifer in southeast Egypt. Journal of Environmental Geology, 43, 188-196.

Ebraheem, A.M., Garamoon, H.K., Said, S., Wycisk, P. & El Nasr, A.M.S (2003). Numerical modeling of groundwater resources management options in the East Oweinat area, SW Egypt. Environmental Geology, 44(4), 433-447.

Elkrail, A.B. & Obied, B.A. (2013). Hydrochemical characterization and groundwater quality in Delta Tokar alluvial plain, Red Sea coast, Sudan. Arabian Journal of Geosciences, 6, 3133-3138.

Elsheikh, A.E. (2015). Mitigation of groundwater level deterioration of the Nubian Sandstone aquifer in Farafra Oasis, Western Desert, Egypt. Environmental Earth Sciences, 74(3), 2351-2367.

Farrag, A.A., Megahed, H.A. & Darwish, M.H. (2019). Remote sensing, GIS and chemical analysis for assessment of environmental impacts on rising of groundwater around Kima Company, Aswan, Egypt. Bulletin of the National Research Centre, 43(14), 1-14.

Freeze, R.A. & Cherry, J.A. (1979). Groundwater. Prentice-Hall Inc., Englewood Cliffs, Vol. 7632, 604.

Freundlich, H.M.F. (1906). Uber die adsorption in Losungen [Over the adsorption in solution]. Z. Phys. Chem., 57, 385-470.

Galal, W.F. & Darwish, M.H. (2020). Geoenvironmental assessment of the mut wastewater ponds in the Dakhla Oasis, Egypt. Geocarto International. doi. 10.1080/10106049.2020.1856197.

Hem, J.D. (1970). Study and Interpretation of the Chemical Characteristics of Natural Water. Second Edition, U.S. Geological Survey Water Supply Paper, 1473, p.363.

Hem, J.D. (1989). Study and Interpretation of the Chemical Characteristics of Natural Water. U.S. Geological Survey Water Supply Paper, 2254, p.264.

Hermina M.H. (1990). The surrounding of Kharga, Dakhla and Farafra oases. In: Said, R. (Ed.). The geology of Egypt. Balkema, Rotterdam, Brookfield, the Netherlands, Ch.14, p.295-292.

Ho, Y.S. & Mckay, G. (1999). Psuedo-second order model for sorption processes. Process biochemistry, 34, 451-465.

Holman, I.P., Whelan, M.J., Howden, N.J.K., Bellamy, P.H., Willby, N.J., Rivas-Casado, M. & McConvey, P. (2008). Phosphorus in groundwater – An overlooked contributor to eutrophication. Hydrological Processes, 22, 5121-5127.

Husein, D.Z. (2013). Adsorption and removal of mercury ions from aqueous solution using raw and chemically modified Egyptian mandarin peel. Desalination and Water Treatment, 51, 6761-6769.

Husein, D.Z. (2019). Facile one-pot synthesis of porous N-doped graphene based NiO composite for parabens removal from wastewater and its reusability. Desalination and Water Treatment, 166, 211-221.

John De Zuane, P.E. (1990). Handbook of Drinking Water Quality-Standards and Controls, Van Nostrand Reinhold: New York; p. 132-134.

Kaitantzian, A., Kelepertzis, E. & Kelepertsis, A. (2013). Evaluation of the sources of contamination in the suburban area of Koropi -Markopoulo, Athens, Greece. Bulletin of Environmental Contamination and Toxicology, 91, 23-28.

Lagergern, S. (1898). About the theory of so-called adsorption of soluble substances. K. Sven. Vetenskapsakad. HANDLINGAR, 24 (4), 1-39.

Langmuir, I. (1918). The adsorption of gases on plane surfaces of glass, mica and platinum. Journal of the American Chemical Society, 40, 1361-1403.

Lee, H., Kim, D., Kim, J., Ji, M.-K., Han, Y.-S., Park, Y.-T., Yun, H.-S. & Choi, J. (2015). As (III) and As (V) removal from the aqueous phase via adsorption onto acid mine drainage sludge (AMDS) alginate beads and goethite alginate beads. Journal of Hazardous Materials, 292, 146-154.

Lee, C., Jung, J., Pawar, R., Kim, M. & Lalhmunsiama, Lee, -M. (2017). Arsenate and phosphate removal from water using Fe-sericite composite beads in batch and fixed-bed systems, Journal of Industrial and Engineering Chemistry, 47, 375-383.

Mahmod, W.E., Watanabe, K. & Zahr-Eldeen, A.A. (2013). Analysis of groundwater flow in arid areas with limited hydrogeological data using the grey model: a case study of the Nubian Sandstone, Kharga Oasis, Egypt. Hydrogeology Journal, 21, 1021-1034.

McRae, S.G. (1972). Glauconite. Earth Science Reviews, 8(4), 397-440.

Mekonnen, D.T., Alemayehu, E. & Lennartz, B. (2020). Removal of Phosphate Ions from Aqueous Solutions by Adsorption onto Leftover Coal. Water, 12, 1381.

Module H.P. (1999). Major ions in water, Hydrology Project, Training module WQ-28. World Bank & Government of the Netherlands funded. New Delhi, India.

Richards, L.A. (1954). Diagnosis and Improvement of Saline Alkali Soils, Agriculture, 160, Handbook 60. US Department of Agriculture, Washington DC.

Selim, K.A., El-Tawil, R.S. & Rostom, M. (2018). Utilization of surface modified phyllosilicate mineral for heavy metals removal from aqueous solutions, Egyptian Journal of Petroleum, 27, 393-401.

Shata, A.A. (1982). Hydrogeology of the great Nubian Sandstone basin, Egypt. Journal of Engineering Geology, 15, 127-133.

Sheila, M. (2005). USGS Water Quality Monitoring, available at http://www.water.usgs.gov/nawqa/circ-1136.html

Singla, R., Alex, T.C. & Kumar, R. (2020). On mechanical activation of glauconite: Physicochemical changes, alterations in cation exchange capacity and mechanisms, Powder Technology, 360, 337-351.

Spraill, T.B., Harned, D.A., Ruhl, P.M., Eimers, J.L., McMahon, G., Smith, K.F., Galeone, D.R. & Woodside, M.D. (1998). U.S. Geological Survey Circular 1157; online at URL:http://water.usgs.gov/pubs/circ.1157.

Temkin, M.I. & Pyzhev, V. (1940). Kinetics of ammonia synthesis on promoted iron catalysts. Acta physicochimica, URSS, 12, 217-222.

Todd, D.K. (1980). Groundwater Hydrology. Second Edition, John Wiley & Sons, New York.

U.S. Salinity Laboratory Staff (1954). Diagnosis and improvement of saline and alkali soils. US Department of Agriculture Handbook 60, Washington, DC.

U.S. Public Health Service (1962). Drinking water standards, U.S. Department of Health, Education and Welfare, Washington, D.C. p.61.

Voss, C.I. & Soliman, S.M. (2014). The transboundary non-renewable Nubian aquifer system of Chad, Egypt, Libya and Sudan: classical groundwater questions and parsimonious hydrogeologic analysis and modeling. Hydrogeology Journal, 22, 441-468.

White (1963). Data of Geochemistry. Chapter F. Chemical Composition. U.S. Geological Survey Water Supply Paper No. 440-F.

World Health Organization (1979). Sodium, chlorides and conductivity in drinking water. EURO reports and studies. No. 2. Copenhagen, Denmark: WHO Regional Office for Europe.